

Multifold behavior of the information transmission by the quantum 3-switch

Lorenzo M. Procopio ^{*†,1} Francisco Delgado,² Marco Enríquez,² and Nadia Belabas¹

¹*Centre for Nanoscience and Nanotechnology, C2N, CNRS,
Université Paris-Sud, Université Paris-Saclay, 91120 Palaiseau, France*

²*School of Engineering and Sciences, Tecnológico de Monterrey,
Carretera a Lago de Guadalupe km. 3.5, Atizapán, Estado de México, México, CP. 52926*

We uncover new behaviors of the transmission of information by three quantum channels in superposition of causal orders subject to some level of noise. We find that the transmission can exhibit three different behaviors as the level of noise is varied. This multifold behavior can be explained by the different equivalence classes of quantum switch matrices related to specific combinations of causal orders. We classify these matrices using their characteristic polynomials and matrix invariants, and we calculate analytical expressions for the Holevo information in three representative cases. Our results are a step forward to understand and harness quantum control of causal orders with different levels of noise. We also study the Holevo information as function of a continuous order parameter and analyse transitions at integer values.

I. INTRODUCTION

In the standard quantum information theory [1], the connections between quantum channels in a network are considered to be classical. In this context the quantum channels are applied in a fixed order in time and in space, i.e., one channel is applied after the next in a sequential way and in a definite order. However, it has been shown recently that quantum channels can be in a superposition of trajectories in space [2] or time [3]. This latter superposition is known as a quantum switch [4] and it has been shown to be an useful resource for new applications in quantum discrimination of channels [5], quantum computation [4], quantum communication complexity [6], quantum channel identification [7], quantum metrology [8] and quantum thermodynamics [9]. Those theoretical investigations have motivated experimental demonstrations of the quantum switch with single photons for two operations [10–13] and more recently with more than two operations [14].

In this new paradigm, the transmission of classical and quantum information using the quantum switch has been theoretically investigated [15–24]. Some experimental tests have also been realized to measure the performances of indefinite causal order in communication theory [25–27]. It has been shown in particular that if one places two fully noisy and identical quantum channels in a superposition of causal orders, the transmission of classical information is non-zero [15]. This effect was an unexpected result that can be understood as the interference of two noisy processes using non-commuting operators which can reduce the level of noise. For more than two channels, investigations on the transmission of information with three [18] or more channels [17, 22–24] have shown communication advantages in a multi-party scenario. While [22–24] are mainly concerned with the transmission of information of N fully noisy channels and are limited to N cyclic orders of channels, in [17] a general expression for the action of the quantum switch with N channels considering the complete set of permutations and any level of noise was given. In this last approach, interesting specific combinations of channel orders can be obtained when properly restricting the initial form of the control state or after post-selection. In the present work, we exploit the method developed in [17] to uncover new behaviors of the transmission of classical information subjected to some arbitrary level of noise. We found indeed, that in the case of three channels, different equivalence classes of combinations of causal orders exhibit different behaviors of the transmission of information as the degree of depolarization increases. We show here that these behaviors can be associated to different classes of equivalence matrices for the quantum switch. We classify those matrices and show that some of those classes of matrices are more efficient than others to transmit information for any degree of noise. Our classification simplifies the calculation of the information of Holevo for all possible combinations of causal orders with three channels. We calculate some representative cases to show the usefulness of our method. Our analytical results not only confirm our numerical results reported in the fully noisy channel case [18], but give a formal description of control of causal orders for any level of noise.

The structure of the paper is as follows. In section II, we review the basic concepts to study the transmission of classical information with three noisy channels in superposition of causal orders. Then in section III we classify all the quantum switch matrices for any combination of cyclic and non-cyclic orders of channels. Furthermore we calculate

* Corresponding author: lorenzo.procopio@weizmann.ac.il

† Current address: Weizmann Institute of Science, Rehovot 7610001, Israel

explicitly the Holevo information in representative cases, i.e., for a superposition of three cyclic orders ($m = 3$) and for a superposition of all the causal orders ($m = 6$). In section V, we extend the concept of number of causal orders m into the continuum, thus defining a fractional causal order for the Holevo information. Finally, in Section VI we give our conclusions and perspectives.

II. THE QUANTUM 3-SWITCH

We model the action of a noisy channel \mathcal{N} on a qudit (d -dimensional) system ρ as a stochastic depolarizing quantum channel

$$\mathcal{N}(\rho) = q\rho + (1 - q)\text{Tr}[\rho]\frac{\mathbf{1}}{d} \quad (1)$$

where $\mathbf{1}$ is the identity operator. It yields a maximally mixed state $\mathbf{1}$ for the target system when the channel is fully-noisy, i.e., $q = 0$. For $q \neq 0$, the channel \mathcal{N} is partially depolarizing and it becomes transparent for $q = 1$. We study the transmission of classical information for the case when the quantum channels are identical with arbitrary depolarizing parameter q . We use the Kraus decomposition $\mathcal{N}(\rho) = \sum_i K_i \rho K_i^\dagger$ to mathematically represent the action of a channel \mathcal{N} on the quantum state ρ with $\sum_i K_i K_i^\dagger = \mathbf{1}$. For three noisy channels \mathcal{N}_1 , \mathcal{N}_2 and \mathcal{N}_3 , the input control system $\rho_c = |\psi_c\rangle\langle\psi_c|$ uses $3!$ states to coherently control the target system ρ , where $|\psi_c\rangle = \sum_{n=1}^6 \sqrt{P_k} |k\rangle$, with $\sum_{k=1}^6 P_k = 1$. These states encode six configurations where the three channels are applied in a definite causal order: if ρ_c is in the state $|1\rangle$, then the order to apply the channels will be $\mathcal{N}_1 \circ \mathcal{N}_2 \circ \mathcal{N}_3$. Likewise, if ρ_c is in the states $|2\rangle$, $|3\rangle$, $|4\rangle$, $|5\rangle$ or $|6\rangle$, the orders will be $\mathcal{N}_1 \circ \mathcal{N}_3 \circ \mathcal{N}_2$, $\mathcal{N}_2 \circ \mathcal{N}_1 \circ \mathcal{N}_3$, $\mathcal{N}_2 \circ \mathcal{N}_3 \circ \mathcal{N}_1$, $\mathcal{N}_3 \circ \mathcal{N}_1 \circ \mathcal{N}_2$ and $\mathcal{N}_3 \circ \mathcal{N}_2 \circ \mathcal{N}_1$ respectively. By setting the control state $|\psi_c\rangle$ in a superposition, all causal orders can be applied simultaneously. We refer to this type of superposition as the quantum 3-switch which is an extension of the quantum 2-switch with new partial ways to coherently control quantum channels in space and time [18].

If the Kraus operators of the channels \mathcal{N}_1 , \mathcal{N}_2 and \mathcal{N}_3 are $\{K_i^{(1)}\}$, $\{K_j^{(2)}\}$ and $\{K_k^{(3)}\}$ respectively, then the Kraus operators \mathcal{K}_{ijk} of the full quantum channel obtained by superimposing the three channels in a causal order becomes $\mathcal{K}_{ijk} = \sum_n \pi_n (K_i^{(1)} K_j^{(2)} K_k^{(3)}) |n\rangle\langle n|$, where π_n is a permutation of the symmetric class $S_N = \{\pi_k | k \in [1; N!]\}$. The full quantum channel resulting from controlling three identical noisy channels in a superposition of causal orders, with depolarizing parameter q , can be written as [17]

$$\mathcal{S}^{(m)} = \frac{1}{m} \begin{pmatrix} mP_1A & \sqrt{\xi_{12}}B & \sqrt{\xi_{13}}B & \sqrt{\xi_{14}}D & \sqrt{\xi_{15}}D & \sqrt{\xi_{16}}F \\ \sqrt{\xi_{12}}B & mP_2A & \sqrt{\xi_{23}}D & \sqrt{\xi_{24}}F & \sqrt{\xi_{25}}B & \sqrt{\xi_{26}}D \\ \sqrt{\xi_{13}}B & \sqrt{\xi_{23}}D & mP_3A & \sqrt{\xi_{34}}B & \sqrt{\xi_{35}}F & \sqrt{\xi_{36}}D \\ \sqrt{\xi_{14}}D & \sqrt{\xi_{24}}F & \sqrt{\xi_{34}}B & mP_4A & \sqrt{\xi_{45}}D & \sqrt{\xi_{46}}B \\ \sqrt{\xi_{15}}D & \sqrt{\xi_{25}}B & \sqrt{\xi_{35}}F & \sqrt{\xi_{45}}D & mP_5A & \sqrt{\xi_{56}}B \\ \sqrt{\xi_{16}}F & \sqrt{\xi_{26}}D & \sqrt{\xi_{36}}D & \sqrt{\xi_{46}}B & \sqrt{\xi_{56}}B & mP_6A \end{pmatrix}, \quad (2)$$

where the matrix elements are given by

$$\begin{aligned} A &= \rho q^3 + \frac{1}{d} (1 - q^3) \\ D &= \frac{\rho}{d^2} ((d^2 + 1) q^3 - q^2 - q + 1) + \frac{1}{d} (-2q^3 + q^2 + q) \\ B &= \frac{q\rho}{d^2} ((d^2 + 1) q^2 - 2q + 1) - \frac{1}{d^3} (q - 1) ((d^2 + 1) q^2 + 2(d^2 - 1) q + 1) \\ F &= \frac{\rho}{d^2} (d^2 q^3 + 3(q - 1)^2 q) + \frac{1}{d^3} ((1 - q)^3 - 3d^2(q - 1)q^2), \end{aligned} \quad (3)$$

where d is the dimension of the target system ρ . We have introduced the parameter $m \in [1; 6]$ which defines the number of non zero P_i s to characterize the corresponding superposition of causal orders. We have also introduced the parameter $\xi_{ij} = m^2 P_i P_j$, which is known as the coherent indefiniteness [7], such that $0 \leq \xi_{ij} \leq 1$, which reflects the degree of superposition between two definite causal orders determined by the control states $|i\rangle\langle i|$ and $|j\rangle\langle j|$. We have a definite order when $\xi_{ij} = 0$ and maximally indefiniteness when $\xi_{ij} = 1$. We see from the quantum switch matrix $\mathcal{S}^{(m)}$ that the dependence on the probabilities P_k enables the exploration of transmission of information via different combinations of m causal orders. Different sets of P_k s at constant m give a different matrix and a different Holevo information analysis. Note that the Holevo information depends completely on the calculation of eigenvalues of the resulting matrix $\mathcal{S}^{(m)}$ and those eigenvalues depend on the set of invariants of the matrix.

In the next section we classify the quantum switch matrices and calculate the Holevo information in some particular cases. To quantify how much classical information can be transmitted through a quantum channel \mathcal{S} , we indeed compute the Holevo information χ as

$$\chi(\mathcal{S}) = \log d + H(\tilde{\rho}_c) - H^{\min}(\mathcal{S}), \quad (4)$$

where $H(\tilde{\rho}_c)$ is the von-Neumann entropy of the output control system $\tilde{\rho}_c$ after the channel \mathcal{S} and $H^{\min}(\mathcal{S})$ is the minimum of the entropy at the output of the channel \mathcal{S} [17]. Using the concavity property of entropy, the minimum of the entropy H^{\min} for the output target state $\mathcal{S}(\rho)$ corresponds to a state ρ reached by setting only one of its eigenvalues $\lambda_{\rho,i}$ equal to one ($0 \leq \lambda_{\rho,i} \leq 1$ and $i = 1, \dots, 6$). The eigenvalues of $\lambda_{\mathcal{S}(\rho)}$ will be depicted using two indexes as $\lambda_{s,i}$. Index $s = 1, 2, \dots, 6$ for the control, and index $i = 1, \dots, d$ for the input target state. Because all matrices in the block structure of $\mathcal{S}(\rho)$ are linear combinations of $\mathbf{1}$ and ρ , each block element $\mathcal{S}(\rho)$ has common eigenstates. There is then a one-to-one correspondence between the eigenvalues of ρ and those of each block element $\mathcal{S}(\rho)_i$. As a consequence of the previous remarks, for each $\lambda_{\rho,i} = 1$, while all others are zero, there is only one eigenvalue of $\mathcal{S}(\rho)$ including the complete terms for $\mathbf{1}$ and ρ in each block, while the remaining eigenvalues only include the corresponding term to $\mathbf{1}$. For this reason, it is convenient to replace the index i by $k \in \{0, 1\}$, thus grouping the only two relevant cases: those coming from the $d - 1$ different from zero in $\lambda_{\rho,i}$ ($k = 0$), and the unique being equal to one ($k = 1$), see [17] for details. Thus, we calculate H^{\min} as

$$H^{\min}(\mathcal{S}) = - \sum_{\substack{s=1 \\ k \in \{0,1\}}}^6 (d-1)^{1-k} \lambda_{s,k}^{(m)} \log \left(\lambda_{s,k}^{(m)} \right). \quad (5)$$

superscript (m) is used to indicate the causal order being considered. Besides $H(\tilde{\rho}_c)$ can be computed by direct diagonalization of the matrix $\tilde{\rho}_c$.

III. EQUIVALENCE CLASSES OF QUANTUM SWITCH MATRICES

We generate and classify quantum switch matrices for each causal order m . To do that, because the Holevo information calculation depends on the eigenvalues of the matrix $\mathcal{S}^{(m)}$ and thus of its invariants, we derive the characteristic polynomials and the matrix invariants of the quantum switch matrices for each causal order m .

In Appendix A, we present calculations of eigenvalues for block matrices. We calculate the determinant of matrices consisting of commuting block matrices as the usual determinant for scalar entries. Indeed commuting blocks can be treated as scalars. The coefficients of the characteristic polynomial of such matrices depend only on the block matrices sub-determinants regardless of the arrangement of blocks. So the Holevo information behaviour of each possible quantum switch is the same for a whole class of matrices which will all have the same set of eigenvalues. To classify the matrices and generate representative of each class, we fix m values of probabilities P_k to be $P_k = 1/m$ and the rest of probabilities equal to zero. Note that in general some block entries of matrix (2) become zero matrices, see Appendix B. We systematically present the quantum switch matrices for causal order m , i.e., each integer number of m causal orders involved in ρ_c .

A. Causal order $m = 1$

There are six configurations to combine the three channels in a definite causal order. To take only one configuration, we fix the probability P_k equal to one and the rest of probabilities equal to zero. Doing like this, we have six different matrices, $\mathcal{S}_1^{(1)}$, $\mathcal{S}_2^{(1)}$, $\mathcal{S}_3^{(1)}$, $\mathcal{S}_4^{(1)}$, $\mathcal{S}_5^{(1)}$ and $\mathcal{S}_6^{(1)}$ with only one non-zero matrix element A , and the rest elements are zero, see matrices (B.1) from Appendix B. The characteristic polynomial is $\mathcal{P}^{(1)}(\lambda_k) = \lambda_k^5 (A_k - \mathbf{1}\lambda_k)$. Thus, the eigenvalues of $\mathcal{S}_i^{(1)}$ are obtained directly from A . If A_k is the k -th element in its diagonal representation, then the eigenvalues of $\mathcal{S}^{(1)}$ are $\lambda_{k,1}^{(1)} = A_k$, with $k = 1, 2, \dots, d$.

B. Causal order $m = 2$

For $m = 2$, we have 15 combinations of two non-zero probabilities P_k s to superimpose two definite causal orders. Each pair of P_k s correspond to a special case of the quantum switch matrix (2). In total, we have 15 different quantum switch matrices for $m = 2$ causal orders, see Appendix B. For maximum indefiniteness $\xi_{ij} = 1$, we found that the 15 quantum switch matrices can be classified in three different classes of matrices according to their matrix invariants, see Table I. The matrices of each set are equivalent thus stating classes, so that it is enough to take one element of the class to make predictions on the transmission of information. The following matrices are the quantum switch matrices that represent the classes 1, 2 and 3 respectively:

$$\begin{aligned}
S_1^{(2)} &= \frac{1}{2} \begin{pmatrix} A & B & 0 & 0 & 0 & 0 \\ B & A & 0 & 0 & 0 & 0 \\ 0 & 0 & 0 & 0 & 0 & 0 \\ 0 & 0 & 0 & 0 & 0 & 0 \\ 0 & 0 & 0 & 0 & 0 & 0 \\ 0 & 0 & 0 & 0 & 0 & 0 \end{pmatrix}, & S_3^{(2)} &= \frac{1}{2} \begin{pmatrix} A & 0 & 0 & D & 0 & 0 \\ 0 & 0 & 0 & 0 & 0 & 0 \\ 0 & 0 & 0 & 0 & 0 & 0 \\ D & 0 & 0 & A & 0 & 0 \\ 0 & 0 & 0 & 0 & 0 & 0 \\ 0 & 0 & 0 & 0 & 0 & 0 \end{pmatrix}, \\
S_5^{(2)} &= \frac{1}{2} \begin{pmatrix} A & 0 & 0 & 0 & 0 & F \\ 0 & 0 & 0 & 0 & 0 & 0 \\ 0 & 0 & 0 & 0 & 0 & 0 \\ 0 & 0 & 0 & 0 & 0 & 0 \\ 0 & 0 & 0 & 0 & 0 & 0 \\ F & 0 & 0 & 0 & 0 & A \end{pmatrix},
\end{aligned} \tag{6}$$

whose characteristic equations can be found in Appendix C 1. Figure 1 shows the Holevo information for each causal order class for $m = 2, 3, \dots, 5$ as the level of noise q_i is varied and $d = 2$. There, for $m = 2$ in Figure 1a, two initial values of the Holevo information split in three different curves as the depolarization strength increases. The three curves are converging to only one value at $q_i = 1$ (not shown), see [17]. Each different behavior in the transmission of information can be associated to one class of the quantum switch matrices. For the initial maximum value of the Holevo information $\chi_{Q3S}^{m=2}$, there is only one equivalence class of quantum switch matrices for which the transmission of information is maximum at $q = 0$. Those matrices correspond to class 2. For this class, the transmission of information is maximum in the region $0 < q_i < 0.5$. For the initial zero value of transmission, there are two different classes of quantum switch matrices showing this value: class 1 and class 3. In these classes, the transmission of information increases as the level of noise decreases. Notice that the quantum switch matrices of class 2 are more efficient to transmit information than matrices of class 3.

C. Causal order $m = 3$

For $m = 3$ causal orders, we have 20 different quantum switch matrices which correspond to the 20 combinations of three non-zero probabilities P_k . The following matrices are the representatives of the classes 1, 2 and 3 respectively:

$$\begin{aligned}
S_1^{(3)} &= \frac{1}{3} \begin{pmatrix} A & B & B & 0 & 0 & 0 \\ B & A & D & 0 & 0 & 0 \\ B & D & A & 0 & 0 & 0 \\ 0 & 0 & 0 & 0 & 0 & 0 \\ 0 & 0 & 0 & 0 & 0 & 0 \\ 0 & 0 & 0 & 0 & 0 & 0 \end{pmatrix}, & S_2^{(3)} &= \frac{1}{3} \begin{pmatrix} A & B & 0 & D & 0 & 0 \\ B & A & 0 & F & 0 & 0 \\ 0 & 0 & 0 & 0 & 0 & 0 \\ D & F & 0 & A & 0 & 0 \\ 0 & 0 & 0 & 0 & 0 & 0 \\ 0 & 0 & 0 & 0 & 0 & 0 \end{pmatrix}, \\
S_8^{(3)} &= \frac{1}{3} \begin{pmatrix} A & 0 & 0 & D & D & 0 \\ 0 & 0 & 0 & 0 & 0 & 0 \\ 0 & 0 & 0 & 0 & 0 & 0 \\ D & 0 & 0 & A & D & 0 \\ D & 0 & 0 & D & A & 0 \\ 0 & 0 & 0 & 0 & 0 & 0 \end{pmatrix},
\end{aligned} \tag{7}$$

whose characteristic equation and eigenvalues can be found in Appendix C 2. Figure 1b shows the Holevo information as the level of noise is varied for $m = 3$. We found that there are also two initial values for Holevo information as we saw for the case of $m = 2$. For this case, however, both initial values are non-zero. We found that only one class of quantum switch matrices has the maximum initial value of χ_{Q3S} . We identified this set of matrices as class 3 (see Appendix C 2). The transmission of information is always maximum for this class and the initial value does not split in more classes of combinations of causal orders. In this case, we report analytical expressions for the eigenvalues of

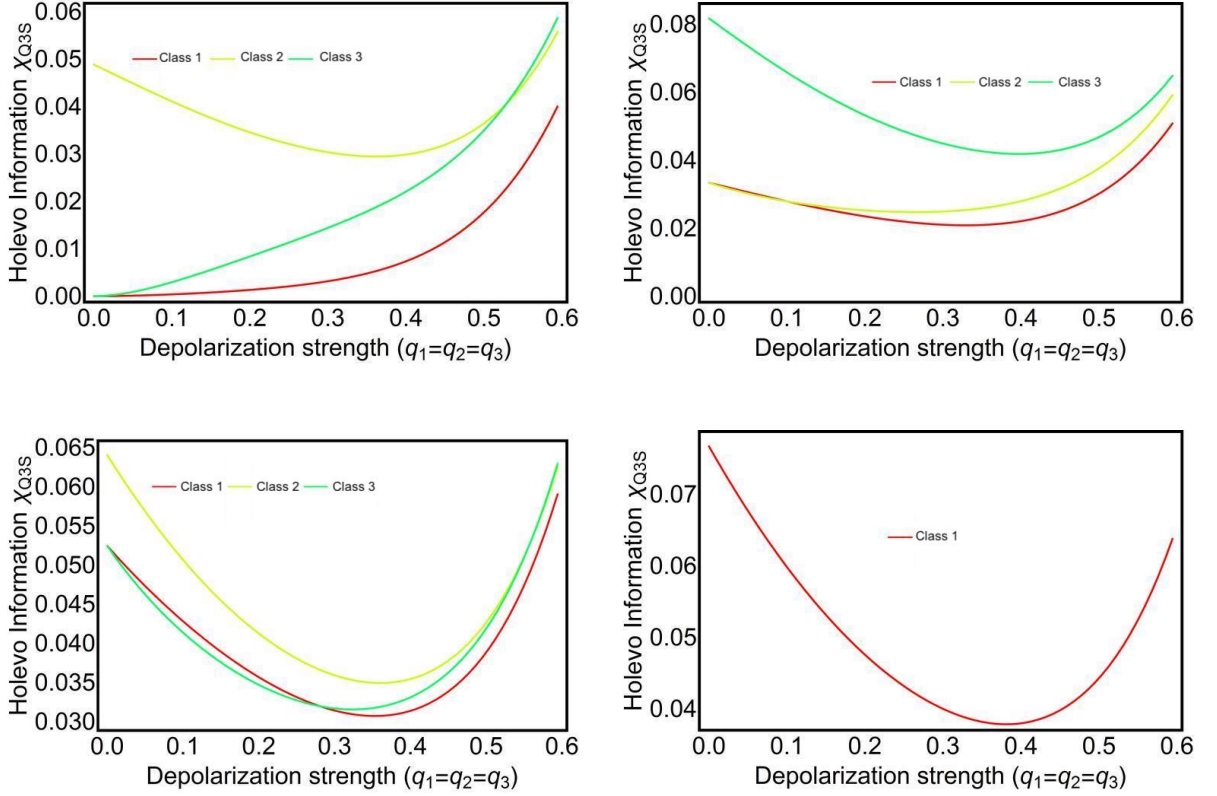


FIG. 1: Holevo information χ_{Q3S} for $N = 3$ channels in indefinite causal order versus the depolarizing strengths q_i for the classes of orders featured by their set of invariants in each order. The graphics from (a)-(d) correspond to the causal order from $m=2$ to $m=5$ respectively. We have labeled each curve with the corresponding equivalence class of the quantum switches matrices, see Table I

$\mathcal{S}_3^{(3)}$ as follows

$$\begin{aligned}\lambda_{k,1}^{(3)} &= \lambda_{k,2}^{(3)} = \frac{1}{3d^2} [(d-k)(q-1^2)(q+1)], \\ \lambda_{k,3}^{(3)} &= \frac{1}{3d^2} [3d^2 k q^3 + d(-5q^3 + 2q^2 + 2q + 1) + 2k(q-1)^2(q+1)], \\ \lambda_{k,j}^{(3)} &= 0, \quad j = 4, 5, 6\end{aligned}\tag{8}$$

On the other hand, the non vanishing eigenvalues of the matrix $\tilde{\rho}_c$ read

$$\begin{aligned}\lambda_1^{(3)} &= \lambda_2^{(3)} = \frac{(d^2 - 1)(q - 1)^2(q + 1)}{3d^2} \\ \lambda_3^{(3)} &= \frac{1}{3} \left[2q + 1 - \frac{2(q - 1)((d^2 - 1)q^2 + 1)}{d^2} \right].\end{aligned}\tag{9}$$

Thus, Holevo information can be computed using equation (4). Remarkably, when $q = 0$ the results reported in Ref. [24] are retrieved as the set of permutations related to the non vanishing parameters P_1, P_4 and P_5 is cyclic.

For the minimum initial value of χ_{Q3S} , the Holevo information is split in two different behaviors as the level of noise is varied. These behaviors are associated to two different classes of quantum switch matrices. We identify these classes as class 1 and 2. In class 1, we found six quantum switch matrices while in class 2, there are 12 switch matrices associated to the same transmission of information. From Figure 1b we can also see that class 1 is less efficient than the other classes to transmit information in the region $0.1 < q_i < 0.6$.

D. Causal order $m = 4$

For $m = 4$ causal orders, we have 15 quantum switch matrices which can be classified in three equivalence classes of matrices described for $m = 2$ and $m = 3$ causal orders. The following matrices are the representatives of the classes 1, 2 and 3 respectively:

$$\begin{aligned}
 S_1^{(4)} &= \frac{1}{4} \begin{pmatrix} A & B & B & D & 0 & 0 \\ B & A & D & F & 0 & 0 \\ B & D & A & B & 0 & 0 \\ D & F & B & A & 0 & 0 \\ 0 & 0 & 0 & 0 & 0 & 0 \\ 0 & 0 & 0 & 0 & 0 & 0 \end{pmatrix}, \quad S_3^{(4)} = \frac{1}{4} \begin{pmatrix} A & B & B & 0 & 0 & F \\ B & A & D & 0 & 0 & D \\ B & D & A & 0 & 0 & D \\ 0 & 0 & 0 & 0 & 0 & 0 \\ 0 & 0 & 0 & 0 & 0 & 0 \\ F & D & D & 0 & 0 & A \end{pmatrix}, \\
 S_5^{(4)} &= \frac{1}{4} \begin{pmatrix} A & B & 0 & D & 0 & F \\ B & A & 0 & F & 0 & D \\ 0 & 0 & 0 & 0 & 0 & 0 \\ D & F & 0 & A & 0 & B \\ 0 & 0 & 0 & 0 & 0 & 0 \\ F & D & 0 & B & 0 & A \end{pmatrix},
 \end{aligned} \tag{10}$$

whose characteristic equation and eigenvalues can be found in Appendix C 3. Figure 1c shows the Holevo information for $m = 4$ causal orders as the level of noise is varied. For this case, we found that the two initial values of the Holevo information are different from zero but less advantageous than the initial values of the case with $m = 3$ causal orders. Class 1 has the maximum transmission of information in the region $0 \leq q \leq 0.5$. In this class there are six equivalence matrices. For the minimum initial value of the Holevo information, we found that there are two classes of matrices giving this value: class 2 and 3. We found that the class 2 has six equivalence switch matrices while class 3 has three.

E. Causal order $m = 5$

For $m = 5$ causal orders, there are six different permutations of five non-zero probabilities P_k , which correspond to six equivalence quantum switch matrices. We found only one class of equivalence matrices. The following matrix can be the representative of the unique class:

$$S_1^{(5)} = \frac{1}{5} \begin{pmatrix} A & B & B & D & D & 0 \\ B & A & D & F & B & 0 \\ B & D & A & B & F & 0 \\ D & F & B & A & D & 0 \\ D & B & F & D & A & 0 \\ 0 & 0 & 0 & 0 & 0 & 0 \end{pmatrix}. \tag{11}$$

For this case all quantum switch matrices have the same characteristic equation and eigenvalues (see Appendix C 4). Figure 1c shows the Holevo information for $m = 5$ causal orders as the level of noise is varied. We found only one maximum, at $q = 0$, and one minimum around $q \leq 0.4$.

F. Causal order $m = 6$.

Finally, for $m = 6$ causal orders, we have only one quantum switch matrix:

$$S_1^{(6)} = \frac{1}{6} \begin{pmatrix} A & B & B & D & D & F \\ B & A & D & F & B & D \\ B & D & A & B & F & D \\ D & F & B & A & D & B \\ D & B & F & D & A & B \\ F & D & D & B & B & A \end{pmatrix}, \tag{12}$$

whose characteristic equation and eigenvalues can be found in Appendix C 5. The eigenvalues of (12) can be computed analytically as

$$\begin{aligned}
\lambda_{k,1}^{(6)} &= \frac{1}{6d^2}(q-1)^2(3q+1)(d-k), \\
\lambda_{k,2}^{(6)} &= \frac{1}{6d^2}(q-1)^2(3q+1)(d-k), \\
\lambda_{k,3}^{(6)} &= \frac{1}{6d^3}(q-1)^2(d^2 + dk(2-3q) + 3(q-1)), \\
\lambda_{k,4}^{(6)} &= -\frac{1}{6d^2}(q-1)^3(d-k), \\
\lambda_{k,5}^{(6)} &= -\frac{1}{6d^2}(q-1)^3(d-k), \\
\lambda_{k,6}^{(6)} &= \frac{1}{6d^3} [6d^3kq^3 + d^2(-10q^3 + 3q^2 + 6q + 1) \\
&\quad + dk(7q+2)(q-1)^2 - 3(q-1)^3].
\end{aligned} \tag{13}$$

On the other hand, the eigenvalues of the matrix $\tilde{\rho}_c$ read

$$\begin{aligned}
\lambda_1^{(6)} &= \alpha + \beta - \gamma - \delta, \\
\lambda_2^{(6)} &= \alpha + \beta - \gamma - \delta, \\
\lambda_3^{(6)} &= \alpha - 2\beta + 2\gamma - \delta, \\
\lambda_4^{(6)} &= \alpha - \beta - \gamma + \delta, \\
\lambda_5^{(6)} &= \alpha - \beta - \gamma + \delta, \\
\lambda_6^{(6)} &= \alpha + 2\beta + 2\gamma + \delta,
\end{aligned} \tag{14}$$

where

$$\alpha = \frac{1}{6}(q^3 + 3q^2(1-q) + (1-q)^3 + 3q(1-q)^2), \tag{15}$$

$$\beta = \frac{1}{6d^2}(d^2q^3 + 3d^2q^2(1-q) + 2d^2q(1-q)^2 + (1-q)^3 + q(1-q)^2), \tag{16}$$

$$\gamma = \frac{1}{6d^2}(d^2q^3 + 3d^2q^2(1-q) + d^2q(1-q)^2 + (1-q)^3 + 2q(1-q)^2), \tag{17}$$

$$\delta = \frac{1}{6d^2}(d^2q^3 + 3d^2q^2(1-q) + (1-q)^3 + 3q(1-q)^2). \tag{18}$$

Accordingly, the Holevo information (4) is computed analytically. For $q = 0$ the previously reported value in [17] is retrieved. A non-zero Holevo information even when the channels are maximally noisy is not intuitive. Equations (2) and (3) indeed show how the output of the quantum switch is proportional to linear combinations of the mixed state $\mathbf{1}$ and the target state ρ where the message is encoded. So even when the channels are maximally noisy, i.e., $q=0$, some terms of the quantum state ρ still survive. It has been discussed in the literature that the main ingredient for having a nontrivial resource is the noncommutativity of the Kraus operators, see for example references [15] and [19], giving rise to an interference term that fosters the survival of the quantum state ρ .

IV. HOLEVO INFORMATION FOR DIFFERENT DIMENSIONS

We also investigate the Holevo information as a function of q_i for different dimensions of the target $d = 2, \dots, 6$. In Figure 2, the best class for each m , which gives the largest χ_{Q3S} for $d = 2$ at the beginning of the range of q_i , has been selected and calculated for $d = 3, 4, \dots, 6$. Thus, Figure (2) shows a comparison of χ_{Q3S} as a function of q_i 's for different dimensions. In general, the transmission of information decreases as the dimension of the target state increases in the region of depolarization $0 < q_i < 0.3$. Above this region, the Holevo information starts to increase while the dimension increases.

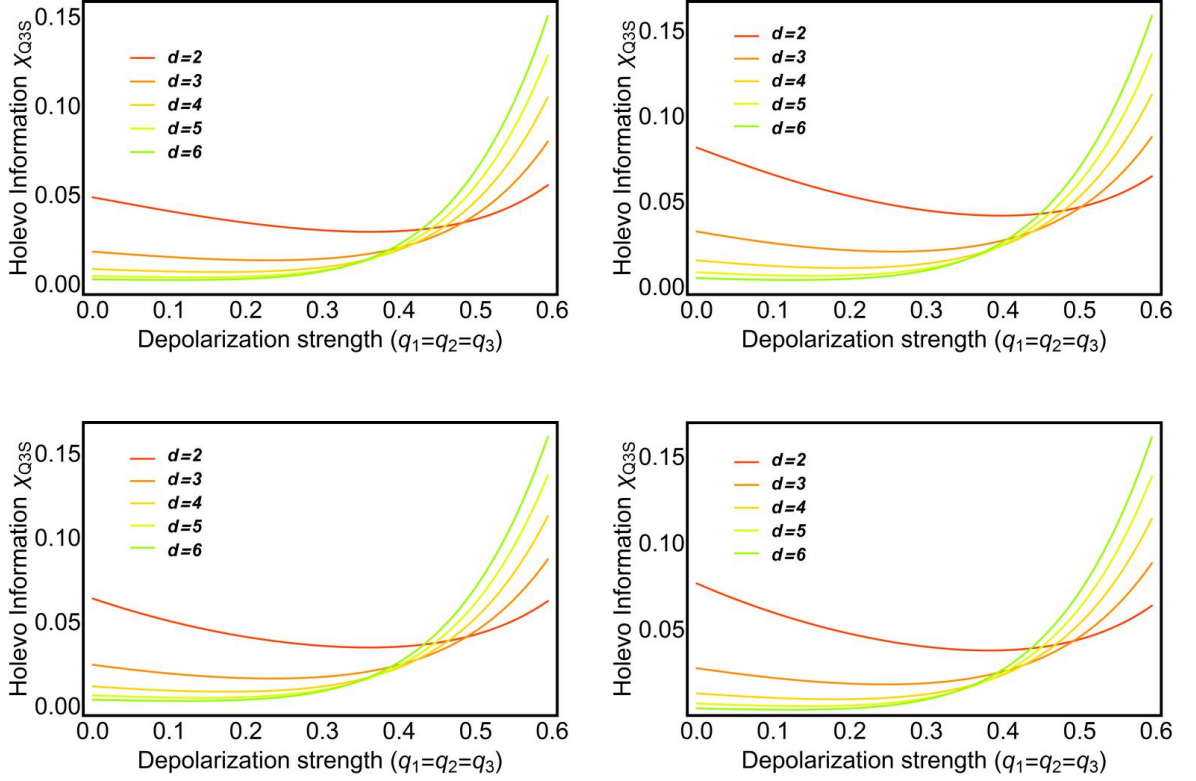


FIG. 2: Holevo information χ_{Q3S} for $N = 3$ channels in indefinite causal order versus the depolarizing strengths q_i as function of dimension $d = 2, \dots, 6$. Holevo information χ_{Q3S} for $N = 3$ channels in indefinite causal order versus the depolarizing strengths q_i as function of dimension $d = 2, \dots, 6$. As in Figure 1, a) to d) corresponds to $m = 2, \dots, 5$. Only one representative class of each $m = 2, \dots, 5$ has been plotted.

V. HOLEVO INFORMATION AS FUNCTION OF A FRACTIONAL CAUSAL ORDER

In this work, we analyse the existence of equivalence classes for the superposition of causal orders introduced in a previous work [17]. m was previously defined as the integer number of definite causal orders equiprobably involved in a quantum switch. In this framework a non integer m had no meaning. Nevertheless, in fact integer m is a special case among many initial control states with continuous coefficients. Thus, for each superposition of causal order m in the current approach considering invariants, this suggests to analyse the behavior of the Holevo information as a function of the continuum associated to the complete set of coefficients P_i of the control system. Thus, in order to analyse the behavior of Holevo information χ_{Q3S} depending on the whole set of possible configurations for the three quantum channel orders, we define the following quantity:

$$m \equiv e^{S_2(\{P_k\})}, \text{ with: } S_2(\{P_k\}) = -\log \sum_{k=1}^{N!} P_k^2 \quad (19)$$

defined in terms of the Renyi's entropy of order 2 [?]. Note that this quantity extends the original definition of a causal order m where a subset of m values of P_k is different from zero and describes an equiprobable configuration, i.e., $P_k = 1/m$. It is a continuous generalization of the causal order concept with integer m as is common for discrete indexes extended into a continuum. Clearly, if m still is an integer, other causal orders with non-zero and equiprobable coefficients are present (it means, with a lower or null set of $P_i = 0$ as is being mainly considered). Thus, the previous causal order definition (19) works as a kind of fractional order for our purposes, letting us analyze χ_{Q3S} (and the invariants) on the whole spectrum of causal orders as a continuum for the general case. We are interested in the discrete transitions found in the previous development stated by the sets of invariants.

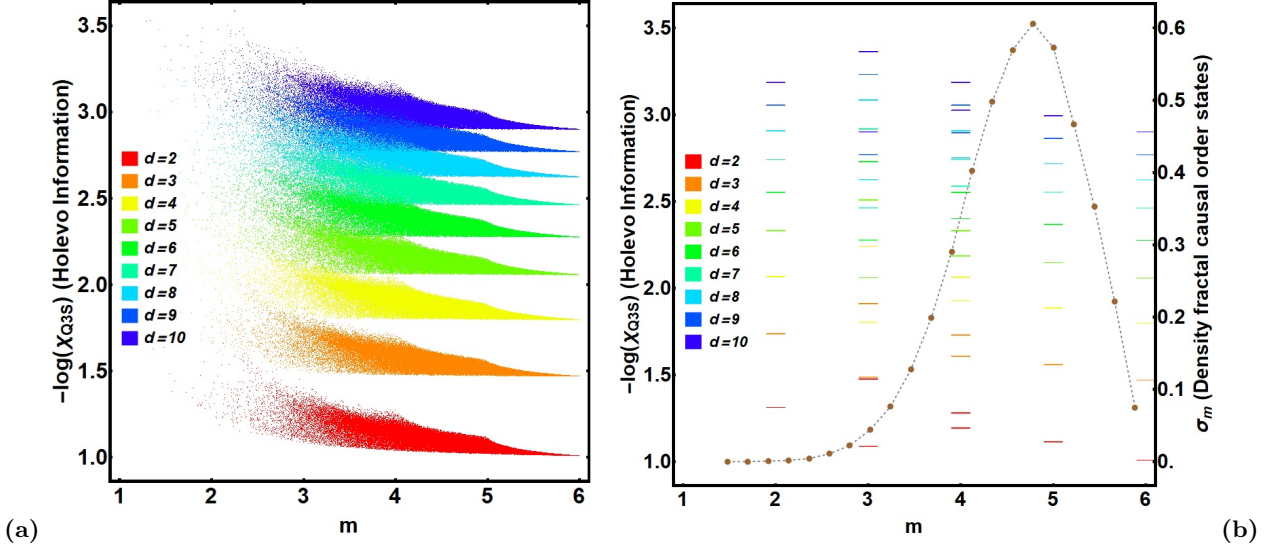


FIG. 3: Holevo information (in a log-scale): a) as function of fractional order m for 10^6 uniform random configurations of $\{P_k\}$ for each $d = 2, 3, \dots, 10$ in totally depolarizing channels ($q_i = 0, i = 1, 2, 3$); and b) for the integer causal orders and their classes in the previous sections together with the statistical distribution σ_m of the fractional order states in a)-dashed line.

Thus, Figure 3a shows the Holevo information χ_{Q3S} (in a log-scale) for totally depolarizing channels ($q_1 = q_2 = q_3 = 0$) in terms of m generalized as fractional in (19), and d for a set of 10^6 uniform random configurations of $P_k \in [0, 1]$ (for each d value) using the Haar measure on the space settled by such parameters, with the restriction $\sum_k P_k = 1$. Note each plot for different value of d apparently sets disjoint regions for χ_{Q3S} for the larger values of m . While, on other side, all plots should converge to $\chi_{Q3S} = 0$ ($-\log(\chi_{Q3S}) \rightarrow \infty$) while $m \rightarrow 1$ as the channels become totally depolarizing. There, the lower frontier for χ_{Q3S} (the upper frontier for $-\log(\chi_{Q3S})$ in the plot) of each coloured region depicts an interesting boundary depending on m and clearly exhibiting a transition behavior when m crosses integer values m , the transition between sets of invariants for each region on the m axis. This distribution exhibits peaks in those frontiers because some of the integer causal orders change. In fact, for $m = 1$ then $\chi_{Q3S} = 0$ ($-\log(\chi_{Q3S}) \rightarrow \infty$) and for $m = 2$, we still get $\chi_{Q3S} = 0$ ($-\log(\chi_{Q3S}) \rightarrow \infty$) for classes 1 and 3, as it can be seen from the Figures 1a and 2a. From Figures 2b-c, it can be inferred that for $m > 2$ and larger d , the Holevo information χ_{Q3S} drops to zero, thus forming peaks on the fractional causal order distribution near the integer values of m , which are not present for non-integer values of m .

Comparing further, in the Figure 3b, the values for the Holevo information χ_{Q3S} (concretely $-\log(\chi_{Q3S})$) are shown for the case of m integer with discrete lines for each value m , as it was presented and calculated in the previous sections. Their values are read on the left scale. Such values should be compared with the distributions shown in the Figure 3a (clearly, the values with $\chi_{Q3S} = 0$ cannot be shown because of the logarithmic scale being used). All of those values are plotted among the fractional m in Figure 3a as special cases, corresponding in color for m integer and each d value. In that plot, we additionally include, in the background, the statistical distribution σ_m obtained numerically departing from the random sample of states generated for each d . It is surprisingly the same for any d and for any of the fractional orders m on Figure 3a. The range for σ_m should be read on the right scale.

VI. CONCLUSIONS

We have investigated the transmission of information for different levels of noise with three noisy channels. We found that different classes of combinations of causal orders predict different behaviors of the transmission of information as the degree of depolarization increases. We classify those combinations in different classes and show that some of those classes are more efficient than others to transmit information in different regimes of depolarization. We have thus found that the multi-fold behaviour of the transmission of information for three channels is associated to different equivalence classes of the quantum switches matrices. These switch matrices are important as they encapsulate the full formal description of the system. They give all the information about the correlations between the causal orders coherently controlled by the control system and yield the output of the quantum switch for different configurations. In addition, these matrices are practical as they simplify cumbersome calculations via the selection of one element

of the equivalence classes to calculate the Holevo information. Our work is a first step to classify the applications of indefinite causal structures for the transmission of information in different regions of depolarization. Despite recent suggestions that the communication enhancement could be due to superposition of channels [27], there is additional evidence showing that the superposition of causal orders is necessary, for the teleportation channel [28], and general Pauli channels [29] for instance. Both works [28] and [29] include a comparison between the impact of causal order superposition and of sequential application of channels in superposition.

The construction of a fractional parameter, generalizing the integer causal orders in the continuum, i.e., the cases where the control states prescribes superpositions of an integer number of m causal orders, enables to visualize the transition of Holevo information around the integer values of causal orders. In addition, this gives insight on some possible behavior in terms of a more general kind of invariants underlying the continuous case. The peaked lower boundary for the Holevo information values χ_{Q3S} could suggest a bifurcation behavior as those being present in chaos theory when a discrete index is extended into the continuum.

Acknowledgments

L. M. Procopio acknowledges the support of Israel Science Foundation and the European Union's Horizon 2020 research under the Marie Skłodowska-Curie grant agreement No 800306. This work was supported by the Paris Ile-de-France region in the framework of DIM SIRTEQ. Francisco Delgado and Marco Enríquez acknowledge the support of Tecnológico de Monterrey and CONACYT.

-
- [1] Shannon, C. E. A mathematical theory of communication. *Bell system technical journal* **27**, 379–423 (1948).
 - [2] Abbott, A. A., Wechs, J., Horsman, D., Mhalla, M. & Branciard, C. Communication through coherent control of quantum channels. *Quantum* **4**, 333 (2020).
 - [3] Chiribella, G. & Kristjánsson, H. Quantum shannon theory with superpositions of trajectories. *Proceedings of the Royal Society A* **475**, 20180903 (2019).
 - [4] Chiribella, G., D'Ariano, G. M., Perinotti, P. & Vedral, V. Quantum computations without definite causal structure. *Physical Review A* **88**, 022318 (2013).
 - [5] Chiribella, G. Perfect discrimination of no-signalling channels via quantum superposition of causal structures. *Physical Review A* **86**, 040301 (2012).
 - [6] Guérin, P. A., Feix, A., Araújo, M. & Brukner, Č. Exponential communication complexity advantage from quantum superposition of the direction of communication. *Physical Review Letters* **117**, 100502 (2016).
 - [7] Frey, M. Indefinite causal order aids quantum depolarizing channel identification. *Quantum Information Processing* **18**, 96 (2019).
 - [8] Zhao, X., Yang, Y. & Chiribella, G. Quantum metrology with indefinite causal order. *Physical Review Letters* **124**, 190503 (2020).
 - [9] Felce, D. & Vedral, V. Quantum refrigeration with indefinite causal order. *Physical Review Letters* **125**, 070603 (2020).
 - [10] Procopio, L. M. *et al.* Experimental superposition of orders of quantum gates. *Nature communications* **6**, 7913 (2015).
 - [11] Rubino, G. *et al.* Experimental verification of an indefinite causal order. *Science advances* **3**, e1602589 (2017).
 - [12] Goswami, K. *et al.* Indefinite causal order in a quantum switch. *Physical Review Letters* **121**, 090503 (2018).
 - [13] Wei, K. *et al.* Experimental quantum switching for exponentially superior quantum communication complexity. *Physical Review Letters* **122**, 120504 (2019).
 - [14] Taddei, M. M. *et al.* Computational Advantage from the Quantum Superposition of Multiple Temporal Orders of Photonic Gates. *PRX Quantum* **2**, 010320 (2021).
 - [15] Ebler, D., Salek, S. & Chiribella, G. Enhanced communication with the assistance of indefinite causal order. *Physical Review Letters* **120**, 120502 (2018).
 - [16] Chiribella, G. *et al.* Indefinite causal order enables perfect quantum communication with zero capacity channel. *New Journal of Physics* **23**, 033039 (2021).
 - [17] Procopio, L. M., Delgado, F., Enríquez, M., Belabas, N. & Levenson, J. A. Communication enhancement through quantum coherent control of n channels in an indefinite causal-order scenario. *Entropy* **21**, 1012 (2019).
 - [18] Procopio, L. M., Delgado, F., Enríquez, M., Belabas, N. & Levenson, J. A. Sending classical information via three noisy channels in superposition of causal orders. *Physical Review A* **101**, 012346 (2020).
 - [19] Loizeau, N. & Grinbaum, A. Channel capacity enhancement with indefinite causal order. *Physical Review A* **101**, 012340 (2020).
 - [20] Caleffi, M. & Cacciapuoti, A. S. Quantum switch for the quantum internet: Noiseless communications through noisy channels. *IEEE Journal on Selected Areas in Communications* **38**, 575–588 (2020).
 - [21] Goswami, K. & Costa, F. Classical communication through quantum causal structures. *Physical Review A* **103**, 042606 (2021).

- [22] Wilson, M. & Chiribella, G. A diagrammatic approach to information transmission in generalised switches. *arXiv preprint arXiv:2003.08224* (2020).
- [23] Chiribella, G., Wilson, M. & Chau, H.-F. Quantum and classical data transmission through completely depolarizing channels in a superposition of cyclic orders. *arXiv preprint arXiv:2005.00618* (2020).
- [24] Sazim, S., Singh, K. & Pati, A. K. Classical communications with indefinite causal order for n completely depolarizing channels. *arXiv preprint arXiv:2004.14339* (2020).
- [25] Goswami, K., Cao Y., Paz-Silva G. A. Romero, J. & White, A. Increasing communication capacity via superposition of order. *Physical Review Research* **2**, 033292 (2020).
- [26] Guo, Y. *et al.* Experimental transmission of quantum information using a superposition of causal orders. *Physical Review Letters* **124**, 030502 (2020).
- [27] Rubino, G. *et al.* Experimental quantum communication enhancement by superposing trajectories. *Physical Review Research* **3**, 013093 (2021).
- [28] Cardoso-Isidoro, C. and Delgado, F. Symmetries in Teleportation Assisted by N-Channels under Indefinite Causal Order and Post-Measurement. *Symmetry* **12**, 1904 (2020).
- [29] Delgado, F. and Cardoso-Isidoro, C. Performance characterization of Pauli channels assisted by indefinite causal order and post-measurement. *Quantum Information and Computation* **20**, 1261 (2020).

Appendices

Appendix A: Theory of eigenvalues for block matrices

1. Characteristic polynomials

In this subsection we establish the theory to get the eigenvalues of (2) when it is reduced to a specific causal orders as it was previously stated. First we consider the $(n+p)N \times (n+p)N$ square block matrix containing pN rows and columns identically equal to the $N \times N$ zero-matrix $\mathbf{0}$:

$$\mathcal{M}_{n+p} \equiv \begin{pmatrix} \mathcal{M}_n & \mathbf{0}_{nN \times pN} \\ \mathbf{0}_{pN \times nN} & \mathbf{0}_{pN \times pN} \end{pmatrix} = \begin{pmatrix} A_{11} & A_{12} & \dots & A_{1n} & \mathbf{0} & \dots & \mathbf{0} \\ A_{21} & A_{22} & \dots & A_{2n} & \mathbf{0} & \dots & \mathbf{0} \\ \vdots & \ddots & \ddots & \vdots & \vdots & \ddots & \vdots \\ A_{n1} & A_{n2} & \dots & A_{nn} & \mathbf{0} & \dots & \mathbf{0} \\ \mathbf{0} & \mathbf{0} & \dots & \mathbf{0} & \mathbf{0} & \dots & \mathbf{0} \\ \vdots & \ddots & \ddots & \vdots & \vdots & \ddots & \vdots \\ \mathbf{0} & \mathbf{0} & \dots & \mathbf{0} & \mathbf{0} & \dots & \mathbf{0} \end{pmatrix}, \quad (\text{A.1})$$

where $\mathbf{0}_{i \times j}$ is the zero-matrix with i rows and j columns and each A_{ij} is a $N \times N$ square matrix. In addition, we assume in our discussion that $[A_{ij}, A_{kl}] = \mathbf{0}, \forall i, j, k, l \in \{1, 2, \dots, n\}$. In addition, we will have $A_{ii} = A_{jj} \equiv A_0, \forall i, j \in \{1, 2, \dots, n\}$ and $A_{ij} = A_{ji}$. Finally, we will consider that all $A_{ij}, \forall i, j \in \{1, 2, \dots, n\}$ can be simultaneously diagonalized under the same transformation.

Clearly, if $\mathcal{P}^{\mathcal{M}_{n+p}}(\lambda)$ is the characteristic polynomial in λ of \mathcal{M}_{n+p} , then $\mathcal{P}^{\mathcal{M}_{n+p}}(\lambda) = \lambda^p \mathcal{P}^{\mathcal{M}_n}(\lambda)$. Then, in order to analyse the eigenvalues of \mathcal{M}_{n+p} , we can restrict our analysis to \mathcal{M}_n . Considering the eigenvalues equation for \mathcal{M}_n :

$$\begin{pmatrix} A_0 & A_{12} & \dots & A_{1n} \\ A_{12} & A_0 & \dots & A_{2n} \\ \vdots & \ddots & \ddots & \vdots \\ A_{1n} & A_{2n} & \dots & A_0 \end{pmatrix} \begin{pmatrix} v_1 \\ v_2 \\ \vdots \\ v_n \end{pmatrix} = \lambda \begin{pmatrix} v_1 \\ v_2 \\ \vdots \\ v_n \end{pmatrix}, \quad (\text{A.2})$$

which can be written as:

$$\begin{aligned} \mathcal{M}'_n \mathcal{V} &\equiv \begin{pmatrix} A_0 - \lambda \mathbf{1} & A_{12} & \dots & A_{1n} \\ A_{12} & A_0 - \lambda \mathbf{1} & \dots & A_{2n} \\ \vdots & \ddots & \ddots & \vdots \\ A_{1n} & A_{2n} & \dots & A_0 - \lambda \mathbf{1} \end{pmatrix} \begin{pmatrix} v_1 \\ v_2 \\ \vdots \\ v_n \end{pmatrix} = \begin{pmatrix} \mathbf{0}_{N \times 1} \\ \mathbf{0}_{N \times 1} \\ \vdots \\ \mathbf{0}_{N \times 1} \end{pmatrix} \\ &\equiv \mathbf{0}_{nN \times 1}, \end{aligned} \quad (\text{A.3})$$

where $\mathbf{1}$ is the $N \times N$ identity matrix and each v_i is a column vector with N elements. Because all blocks commutes among them, we can manipulate each one as an scalar. Thus, by developing a Gaussian elimination process to transform \mathcal{M}'_n into \mathcal{M}''_n , an upper triangular matrix (without leaving denominators in the process), we get the equivalence eigenvalues equation:

$$\mathcal{M}''_n \mathcal{V} \equiv \begin{pmatrix} A_0 - \lambda \mathbf{1} & A_{12} & \dots & A_{1n} \\ \mathbf{0} & A'_1(\lambda, \{A_{ij}\}) & \dots & A'_{2n}(\lambda, \{A_{ij}\}) \\ \vdots & \ddots & \ddots & \vdots \\ \mathbf{0} & \mathbf{0} & \dots & A'_n(\lambda, \{A_{ij}\}) \end{pmatrix} \begin{pmatrix} v_1 \\ v_2 \\ \vdots \\ v_n \end{pmatrix} = \mathbf{0}_{nN \times 1}, \quad (\text{A.4})$$

which implies $A'_n(\lambda, \{A_{ij}\}) = \mathbf{0}$. In addition, straightforwardly $A'_n(\lambda, \{A_{ij}\}) = \det(\mathcal{M}''_n) = \det(\mathcal{M}'_n)$. This last equation conducts immediately to the characteristic polynomial $\mathcal{P}(\mathcal{M}_n)$ if all matrices $A_{ij}, i < j$ are written in their diagonal form. Thus, if a_{ij_k} is the k -th element of A_{ij} in such representation, we get $\mathcal{P}^{\mathcal{M}_n}(\lambda_k) = A'_n(\lambda, \{a_{ij_k}\}), k \in \{1, 2, \dots, N\}$, a set of N polynomials, each one of order n to reach the nN eigenvalues of \mathcal{M}_n . Each polynomial for the set $(\lambda_k), k \in \{1, 2, \dots, N\}$ can be obtained calculating $\det(\mathcal{M}'_n)$ where each A_{ij} is replaced by a_{ij_k} (the elements in their common diagonal representation). We will use this result to get the eigenvalues of (2) for each causal order by noting that entries of (2) (as block matrix) are linear combinations of $\mathbf{1}$ and ρ , which commute. The entries of equation (2) thus also commute and can be diagonalized simultaneously.

2. Matrix invariants

It is found that for a fixed number of causal orders m , there are different matrices generated as function of $P_i \neq 0$. Nonetheless, switch matrices can be classified into equivalence classes provided that all the elements of the class share the same set of eigenvalues. Elements of the same class can be obtained interchanging rows and columns which does not change the set of eigenvalues. Besides, the characteristic polynomial in each class is the same up to a numeric factor. For a given m the different classes should be distinguished from one another. As the determinants of (2) for every causal order vanishes (except for $m = 6$) and its trace is always 1, we cannot use them as discriminant of classes. Instead, we appeal to an alternative invariant. As it is well know, for a given matrix $M = \{m_{ij}\}$ or order $n \times n$, the set of coefficients for its characteristic polynomial:

$$\mathcal{P}_M(\lambda) = \det(M - \lambda \mathbf{1}) = (-1)^n \lambda^n + \sum_{i=1}^n (-1)^i c_i \lambda^i \quad (\text{A.5})$$

(in our case, $c_1 = 1$) is invariant up a scale factor. Such invariants could be written as:

$$c_k = \sum_{\sigma \in S_N} \sum_{\tau \in A_k} \epsilon(\sigma) \prod_{j=1}^k m_{\tau_j \sigma(\tau_j)} \quad (\text{A.6})$$

where $\sigma(i)$ is the image of such permutation on $i \in \{1, 2, \dots, n\}$. In addition, A_k is the set containing all subsets of $k \leq n$ elements from $\{1, 2, \dots, n\}$ and τ_j is its j -th element if $j \leq k$. ϵ is the function giving the signature of each σ .

Thus, the simplest non-trivial invariant that we could build is obtained as the determinant $c_{m \cdot d}$ of $\mathcal{S}^{(m)}$ removing the rows and columns different from zero in (2) after selecting the order m leaving a set of m elements different to zero in $\{P_1, P_2, \dots, P_6\}$ and putting all them equal to $\frac{1}{m}$. Thus, we analyzed the determinant from the matrix just containing the non-trivial blocks in $\mathcal{S}^{(m)}$ and yielding $c_{m \cdot d}$. We showed $c_{m \cdot d}$ for each pair q, d are characteristic for each class.

Appendix B: Matrices for the quantum 3-switch with m causal orders

Causal orders of order m are characterized by the number m of orderings participating in the superposition. Each integer m has a total number $\frac{N!}{m!(N-m)!}$ of cases, but they are grouped in terms of the different invariants in the matrix (2) given by their respective characteristic polynomials, then determining the values of Holevo information χ_{Q3S} . Each class is achieved by the proper selection of a non-null set of P_i values in the control system. In the following we report the matrices derived from (2) representatives of each class.

$$\begin{aligned}
\text{Class 1 : } \quad S_1^{(2)} &= \frac{1}{2} \begin{pmatrix} A & B & 0 & 0 & 0 & 0 \\ B & A & 0 & 0 & 0 & 0 \\ 0 & 0 & 0 & 0 & 0 & 0 \\ 0 & 0 & 0 & 0 & 0 & 0 \\ 0 & 0 & 0 & 0 & 0 & 0 \\ 0 & 0 & 0 & 0 & 0 & 0 \end{pmatrix}, & S_2^{(2)} &= \frac{1}{2} \begin{pmatrix} A & 0 & B & 0 & 0 & 0 \\ 0 & 0 & 0 & 0 & 0 & 0 \\ B & 0 & A & 0 & 0 & 0 \\ 0 & 0 & 0 & 0 & 0 & 0 \\ 0 & 0 & 0 & 0 & 0 & 0 \\ 0 & 0 & 0 & 0 & 0 & 0 \end{pmatrix}, \\
S_8^{(2)} &= \frac{1}{2} \begin{pmatrix} 0 & 0 & 0 & 0 & 0 & 0 \\ 0 & A & 0 & 0 & B & 0 \\ 0 & 0 & 0 & 0 & 0 & 0 \\ 0 & 0 & 0 & 0 & 0 & 0 \\ 0 & B & 0 & 0 & A & 0 \\ 0 & 0 & 0 & 0 & 0 & 0 \end{pmatrix}, & S_{10}^{(2)} &= \frac{1}{2} \begin{pmatrix} 0 & 0 & 0 & 0 & 0 & 0 \\ 0 & 0 & 0 & 0 & 0 & 0 \\ 0 & 0 & A & B & 0 & 0 \\ 0 & 0 & B & A & 0 & 0 \\ 0 & 0 & 0 & 0 & 0 & 0 \\ 0 & 0 & 0 & 0 & 0 & 0 \end{pmatrix}, \\
S_{14}^{(2)} &= \frac{1}{2} \begin{pmatrix} 0 & 0 & 0 & 0 & 0 & 0 \\ 0 & 0 & 0 & 0 & 0 & 0 \\ 0 & 0 & 0 & 0 & 0 & 0 \\ 0 & 0 & 0 & A & 0 & B \\ 0 & 0 & 0 & 0 & 0 & 0 \\ 0 & 0 & 0 & B & 0 & A \end{pmatrix}, & S_{15}^{(2)} &= \frac{1}{2} \begin{pmatrix} 0 & 0 & 0 & 0 & 0 & 0 \\ 0 & 0 & 0 & 0 & 0 & 0 \\ 0 & 0 & 0 & 0 & 0 & 0 \\ 0 & 0 & 0 & 0 & 0 & 0 \\ 0 & 0 & 0 & 0 & A & B \\ 0 & 0 & 0 & 0 & B & A \end{pmatrix}.
\end{aligned} \tag{B.2}$$

Class 2 :

$$S_3^{(2)} = \frac{1}{2} \begin{pmatrix} A & 0 & 0 & D & 0 & 0 \\ 0 & 0 & 0 & 0 & 0 & 0 \\ 0 & 0 & 0 & 0 & 0 & 0 \\ D & 0 & 0 & A & 0 & 0 \\ 0 & 0 & 0 & 0 & 0 & 0 \\ 0 & 0 & 0 & 0 & 0 & 0 \end{pmatrix}, \quad S_4^{(2)} = \frac{1}{2} \begin{pmatrix} A & 0 & 0 & 0 & D & 0 \\ 0 & 0 & 0 & 0 & 0 & 0 \\ 0 & 0 & 0 & 0 & 0 & 0 \\ 0 & 0 & 0 & 0 & 0 & 0 \\ D & 0 & 0 & 0 & A & 0 \\ 0 & 0 & 0 & 0 & 0 & 0 \end{pmatrix},$$

$$S_6^{(2)} = \frac{1}{2} \begin{pmatrix} 0 & 0 & 0 & 0 & 0 & 0 \\ 0 & A & D & 0 & 0 & 0 \\ 0 & D & A & 0 & 0 & 0 \\ 0 & 0 & 0 & 0 & 0 & 0 \\ 0 & 0 & 0 & 0 & 0 & 0 \\ 0 & 0 & 0 & 0 & 0 & 0 \end{pmatrix}, \quad S_9^{(2)} = \frac{1}{2} \begin{pmatrix} 0 & 0 & 0 & 0 & 0 & 0 \\ 0 & A & 0 & 0 & 0 & D \\ 0 & 0 & 0 & 0 & 0 & 0 \\ 0 & 0 & 0 & 0 & 0 & 0 \\ 0 & 0 & 0 & 0 & 0 & 0 \\ 0 & D & 0 & 0 & 0 & A \end{pmatrix}, \quad (\text{B.3})$$

$$S_{12}^{(2)} = \frac{1}{2} \begin{pmatrix} 0 & 0 & 0 & 0 & 0 & 0 \\ 0 & 0 & 0 & 0 & 0 & 0 \\ 0 & 0 & A & 0 & 0 & D \\ 0 & 0 & 0 & 0 & 0 & 0 \\ 0 & 0 & 0 & 0 & 0 & 0 \\ 0 & 0 & D & 0 & 0 & A \end{pmatrix}, \quad S_{13}^{(2)} = \frac{1}{2} \begin{pmatrix} 0 & 0 & 0 & 0 & 0 & 0 \\ 0 & 0 & 0 & 0 & 0 & 0 \\ 0 & 0 & 0 & 0 & 0 & 0 \\ 0 & 0 & 0 & A & D & 0 \\ 0 & 0 & 0 & D & A & 0 \\ 0 & 0 & 0 & 0 & 0 & 0 \end{pmatrix}.$$

Class 3 :

$$S_5^{(2)} = \frac{1}{2} \begin{pmatrix} A & 0 & 0 & 0 & 0 & F \\ 0 & 0 & 0 & 0 & 0 & 0 \\ 0 & 0 & 0 & 0 & 0 & 0 \\ 0 & 0 & 0 & 0 & 0 & 0 \\ 0 & 0 & 0 & 0 & 0 & 0 \\ F & 0 & 0 & 0 & 0 & A \end{pmatrix}, \quad S_7^{(2)} = \frac{1}{2} \begin{pmatrix} 0 & 0 & 0 & 0 & 0 & 0 \\ 0 & A & 0 & F & 0 & 0 \\ 0 & 0 & 0 & 0 & 0 & 0 \\ 0 & F & 0 & A & 0 & 0 \\ 0 & 0 & 0 & 0 & 0 & 0 \\ 0 & 0 & 0 & 0 & 0 & 0 \end{pmatrix},$$

$$S_{11}^{(2)} = \frac{1}{2} \begin{pmatrix} 0 & 0 & 0 & 0 & 0 & 0 \\ 0 & 0 & 0 & 0 & 0 & 0 \\ 0 & 0 & A & 0 & F & 0 \\ 0 & 0 & 0 & 0 & 0 & 0 \\ 0 & 0 & F & 0 & A & 0 \\ 0 & 0 & 0 & 0 & 0 & 0 \end{pmatrix}.$$

(B.4)

3. Causal order $m = 3$

$$\begin{aligned}
 \text{Class 1 : } \quad S_1^{(3)} &= \frac{1}{3} \begin{pmatrix} A & B & B & 0 & 0 & 0 \\ B & A & D & 0 & 0 & 0 \\ B & D & A & 0 & 0 & 0 \\ 0 & 0 & 0 & 0 & 0 & 0 \\ 0 & 0 & 0 & 0 & 0 & 0 \\ 0 & 0 & 0 & 0 & 0 & 0 \end{pmatrix}, & S_3^{(3)} &= \frac{1}{3} \begin{pmatrix} A & B & 0 & 0 & D & 0 \\ B & A & 0 & 0 & B & 0 \\ 0 & 0 & 0 & 0 & 0 & 0 \\ 0 & 0 & 0 & 0 & 0 & 0 \\ D & B & 0 & 0 & A & 0 \\ 0 & 0 & 0 & 0 & 0 & 0 \end{pmatrix}, \\
 S_5^{(3)} &= \frac{1}{3} \begin{pmatrix} A & 0 & B & D & 0 & 0 \\ 0 & 0 & 0 & 0 & 0 & 0 \\ B & 0 & A & B & 0 & 0 \\ D & 0 & B & A & 0 & 0 \\ 0 & 0 & 0 & 0 & 0 & 0 \\ 0 & 0 & 0 & 0 & 0 & 0 \end{pmatrix}, & S_{16}^{(3)} &= \frac{1}{3} \begin{pmatrix} 0 & 0 & 0 & 0 & 0 & 0 \\ 0 & A & 0 & 0 & B & D \\ 0 & 0 & 0 & 0 & 0 & 0 \\ 0 & 0 & 0 & 0 & 0 & 0 \\ 0 & B & 0 & 0 & A & B \\ 0 & D & 0 & 0 & B & A \end{pmatrix}, \\
 S_{18}^{(3)} &= \frac{1}{3} \begin{pmatrix} 0 & 0 & 0 & 0 & 0 & 0 \\ 0 & 0 & 0 & 0 & 0 & 0 \\ 0 & 0 & A & B & 0 & D \\ 0 & 0 & B & A & 0 & B \\ 0 & 0 & 0 & 0 & 0 & 0 \\ 0 & 0 & D & B & 0 & A \end{pmatrix}, & S_{20}^{(3)} &= \frac{1}{3} \begin{pmatrix} 0 & 0 & 0 & 0 & 0 & 0 \\ 0 & 0 & 0 & 0 & 0 & 0 \\ 0 & 0 & 0 & 0 & 0 & 0 \\ 0 & 0 & 0 & A & D & B \\ 0 & 0 & 0 & D & A & B \\ 0 & 0 & 0 & B & B & A \end{pmatrix}.
 \end{aligned} \tag{B.5}$$

4. Causal order $m = 4$

Class 1 :

$$S_1^{(4)} = \frac{1}{4} \begin{pmatrix} A & B & B & D & 0 & 0 \\ B & A & D & F & 0 & 0 \\ B & D & A & B & 0 & 0 \\ D & F & B & A & 0 & 0 \\ 0 & 0 & 0 & 0 & 0 & 0 \\ 0 & 0 & 0 & 0 & 0 & 0 \end{pmatrix}, \quad S_2^{(4)} = \frac{1}{4} \begin{pmatrix} A & B & B & 0 & D & 0 \\ B & A & D & 0 & B & 0 \\ B & D & A & 0 & F & 0 \\ 0 & 0 & 0 & 0 & 0 & 0 \\ D & B & F & 0 & A & 0 \\ 0 & 0 & 0 & 0 & 0 & 0 \end{pmatrix},$$

$$S_6^{(4)} = \frac{1}{4} \begin{pmatrix} A & B & 0 & 0 & D & F \\ B & A & 0 & 0 & B & D \\ 0 & 0 & 0 & 0 & 0 & 0 \\ 0 & 0 & 0 & 0 & 0 & 0 \\ D & B & 0 & 0 & A & B \\ F & D & 0 & 0 & B & A \end{pmatrix}, \quad S_8^{(4)} = \frac{1}{4} \begin{pmatrix} A & 0 & B & D & 0 & F \\ 0 & 0 & 0 & 0 & 0 & 0 \\ B & 0 & A & B & 0 & D \\ D & 0 & B & A & 0 & B \\ 0 & 0 & 0 & 0 & 0 & 0 \\ F & 0 & D & B & 0 & A \end{pmatrix}, \quad (\text{B.8})$$

$$S_{14}^{(4)} = \frac{1}{4} \begin{pmatrix} 0 & 0 & 0 & 0 & 0 & 0 \\ 0 & A & 0 & F & B & D \\ 0 & 0 & 0 & 0 & 0 & 0 \\ 0 & F & 0 & A & D & B \\ 0 & B & 0 & D & A & B \\ 0 & D & 0 & B & B & A \end{pmatrix}, \quad S_{15}^{(4)} = \frac{1}{4} \begin{pmatrix} 0 & 0 & 0 & 0 & 0 & 0 \\ 0 & 0 & 0 & 0 & 0 & 0 \\ 0 & 0 & A & B & F & D \\ 0 & 0 & B & A & D & B \\ 0 & 0 & F & D & A & B \\ 0 & 0 & D & B & B & A \end{pmatrix}.$$

Class 2 :

$$S_3^{(4)} = \frac{1}{4} \begin{pmatrix} A & B & B & 0 & 0 & F \\ B & A & D & 0 & 0 & D \\ B & D & A & 0 & 0 & D \\ 0 & 0 & 0 & 0 & 0 & 0 \\ 0 & 0 & 0 & 0 & 0 & 0 \\ F & D & D & 0 & 0 & A \end{pmatrix}, \quad S_4^{(4)} = \frac{1}{4} \begin{pmatrix} A & B & 0 & D & D & 0 \\ B & A & 0 & F & B & 0 \\ 0 & 0 & 0 & 0 & 0 & 0 \\ D & F & 0 & A & D & 0 \\ D & B & 0 & D & A & 0 \\ 0 & 0 & 0 & 0 & 0 & 0 \end{pmatrix},$$

$$S_7^{(4)} = \frac{1}{4} \begin{pmatrix} A & 0 & B & D & D & 0 \\ 0 & 0 & 0 & 0 & 0 & 0 \\ B & 0 & A & B & F & 0 \\ D & 0 & B & A & D & 0 \\ D & 0 & F & D & A & 0 \\ 0 & 0 & 0 & 0 & 0 & 0 \end{pmatrix}, \quad S_{10}^{(4)} = \frac{1}{4} \begin{pmatrix} A & 0 & 0 & D & D & F \\ 0 & 0 & 0 & 0 & 0 & 0 \\ 0 & 0 & 0 & 0 & 0 & 0 \\ D & 0 & 0 & A & D & B \\ D & 0 & 0 & D & A & B \\ F & 0 & 0 & B & B & A \end{pmatrix}, \quad (\text{B.9})$$

$$S_{12}^{(4)} = \frac{1}{4} \begin{pmatrix} 0 & 0 & 0 & 0 & 0 & 0 \\ 0 & A & D & F & 0 & D \\ 0 & D & A & B & 0 & D \\ 0 & F & B & A & 0 & B \\ 0 & 0 & 0 & 0 & 0 & 0 \\ 0 & D & D & B & 0 & A \end{pmatrix}, \quad S_{13}^{(4)} = \frac{1}{4} \begin{pmatrix} 0 & 0 & 0 & 0 & 0 & 0 \\ 0 & A & D & 0 & B & D \\ 0 & D & A & 0 & F & D \\ 0 & 0 & 0 & 0 & 0 & 0 \\ 0 & B & F & 0 & A & B \\ 0 & D & D & 0 & B & A \end{pmatrix}.$$

Class 3 :

$$S_5^{(4)} = \frac{1}{4} \begin{pmatrix} A & B & 0 & D & 0 & F \\ B & A & 0 & F & 0 & D \\ 0 & 0 & 0 & 0 & 0 & 0 \\ D & F & 0 & A & 0 & B \\ 0 & 0 & 0 & 0 & 0 & 0 \\ F & D & 0 & B & 0 & A \end{pmatrix}, \quad S_{11}^{(4)} = \frac{1}{4} \begin{pmatrix} 0 & 0 & 0 & 0 & 0 & 0 \\ 0 & A & D & F & B & 0 \\ 0 & D & A & B & F & 0 \\ 0 & F & B & A & D & 0 \\ 0 & B & F & D & A & 0 \\ 0 & 0 & 0 & 0 & 0 & 0 \end{pmatrix},$$

$$S_9^{(4)} = \frac{1}{4} \begin{pmatrix} A & 0 & B & 0 & D & F \\ 0 & 0 & 0 & 0 & 0 & 0 \\ B & 0 & A & 0 & F & D \\ 0 & 0 & 0 & 0 & 0 & 0 \\ D & 0 & F & 0 & A & B \\ F & 0 & D & 0 & B & A \end{pmatrix}.$$

(B.10)

5. Causal order $m = 5$

Class 1 :

$$S_1^{(5)} = \frac{1}{5} \begin{pmatrix} A & B & B & D & D & 0 \\ B & A & D & F & B & 0 \\ B & D & A & B & F & 0 \\ D & F & B & A & D & 0 \\ D & B & F & D & A & 0 \\ 0 & 0 & 0 & 0 & 0 & 0 \end{pmatrix}, \quad S_2^{(5)} = \frac{1}{5} \begin{pmatrix} A & B & B & D & 0 & F \\ B & A & D & F & 0 & D \\ B & D & A & B & 0 & D \\ D & F & B & A & 0 & B \\ 0 & 0 & 0 & 0 & 0 & 0 \\ F & D & D & B & 0 & A \end{pmatrix}$$

$$S_3^{(5)} = \frac{1}{5} \begin{pmatrix} A & B & B & 0 & D & F \\ B & A & D & 0 & B & D \\ B & D & A & 0 & F & D \\ 0 & 0 & 0 & 0 & 0 & 0 \\ D & B & F & 0 & A & B \\ F & D & D & 0 & B & A \end{pmatrix}, \quad S_4^{(5)} = \frac{1}{5} \begin{pmatrix} A & B & 0 & D & D & F \\ B & A & 0 & F & B & D \\ 0 & 0 & 0 & 0 & 0 & 0 \\ D & F & 0 & A & D & B \\ D & B & 0 & D & A & B \\ F & D & 0 & B & B & A \end{pmatrix}$$

$$S_5^{(5)} = \frac{1}{5} \begin{pmatrix} A & 0 & B & D & D & F \\ 0 & 0 & 0 & 0 & 0 & 0 \\ B & 0 & A & B & F & D \\ D & 0 & B & A & D & B \\ D & 0 & F & D & A & B \\ F & 0 & D & B & B & A \end{pmatrix}, \quad S_6^{(5)} = \frac{1}{5} \begin{pmatrix} 0 & 0 & 0 & 0 & 0 & 0 \\ 0 & A & D & F & B & D \\ 0 & D & A & B & F & D \\ 0 & F & B & A & D & B \\ 0 & B & F & D & A & B \\ 0 & D & D & B & B & A \end{pmatrix}$$

(B.11)

6. Causal order $m = 6$

Class 1 :

$$\mathcal{S}^{(6)} = \frac{1}{6} \begin{pmatrix} A & B & B & D & D & F \\ B & A & D & F & B & D \\ B & D & A & B & F & D \\ D & F & B & A & D & B \\ D & B & F & D & A & B \\ F & D & D & B & B & A \end{pmatrix},$$

(B.12)

The following table summarizes the equivalence classes of quantum switches matrices:

| | $m = 1$ | $m = 2$ | $m = 3$ | $m = 4$ | $m = 5$ | $m = 6$ |
|---------|--|---|---|---|--|-----------|
| Class 1 | $S_1^{(1)}$ $S_2^{(1)}$ $S_3^{(1)}$ $S_4^{(1)}$ $S_5^{(1)}$ $S_6^{(1)}$ | $S_1^{(2)}$ $S_2^{(2)}$ $S_8^{(2)}$ $S_{10}^{(2)}$ $S_{14}^{(2)}$ $S_{15}^{(2)}$ | $S_1^{(3)}$ $S_3^{(3)}$ $S_5^{(3)}$ $S_{16}^{(3)}$ $S_{18}^{(3)}$ $S_{20}^{(3)}$ | $S_1^{(4)}$ $S_3^{(4)}$ $S_6^{(4)}$ $S_8^{(4)}$ $S_{14}^{(4)}$ $S_{15}^{(4)}$ | $S_1^{(5)}$ $S_2^{(5)}$ $S_3^{(5)}$ $S_4^{(5)}$ $S_5^{(5)}$ $S_6^{(5)}$ | $S^{(6)}$ |
| Class 2 | | $S_3^{(2)}$ $S_4^{(2)}$ $S_6^{(2)}$ $S_9^{(2)}$ $S_{12}^{(2)}$ $S_{13}^{(2)}$ | $S_2^{(3)}$ $S_4^{(3)}$ $S_6^{(3)}$ $S_7^{(3)}$ $S_9^{(3)}$ $S_{10}^{(3)}$ $S_{11}^{(3)}$ $S_{12}^{(3)}$ $S_{14}^{(3)}$ $S_{15}^{(3)}$ $S_{17}^{(3)}$ $S_{19}^{(3)}$ | $S_3^{(4)}$ $S_4^{(4)}$ $S_7^{(4)}$ $S_{10}^{(4)}$ $S_{12}^{(4)}$ $S_{13}^{(4)}$ | | |
| Class 3 | | $S_5^{(2)}$ $S_7^{(2)}$ $S_{11}^{(2)}$ | $S_8^{(3)}$ $S_{13}^{(3)}$ | $S_5^{(4)}$ $S_9^{(4)}$ $S_{11}^{(4)}$ | | |

TABLE I: **Table of equivalence classes of quantum switches matrices.** The multi-fold behaviour of the transmission of information for three channels is associated to these equivalence classes of the quantum switches matrices. We have plotted the curves in Figure 1 for a representative of the class

Appendix C: Characteristic equations from quantum 3-switch matrices

1. Causal order $m = 2$

The characteristic equation from matrices 6 is

$$\mathcal{P}_s^{(2)}(\lambda_k) = \frac{1}{4}\lambda_k^4(A_k - 2\lambda_k - X_k)(A_k - 2\lambda_k + X_k), \quad s = 1, 3, 5 \quad (\text{C.1})$$

where $X = B, D, F$ and their classes of eigenvalues are ($k = 1, 2, \dots, d$ in the following):

$$\begin{aligned} \lambda_{k,1}^{(2)} &= \frac{1}{2}(A_k - X_k), \\ \lambda_{k,2}^{(2)} &= \frac{1}{2}(A_k + X_k), \\ \lambda_{k,j}^{(2)} &= 0, \quad j = 3, \dots, 6. \end{aligned} \quad (\text{C.2})$$

2. Causal order $m = 3$

The characteristic equation for the class 1 of quantum switch matrices with $m = 3$ causal orders is

$$\mathcal{P}_1^{(3)}(\lambda_k) = -\frac{1}{3^3}\lambda_k^3(A_k - D_k - 3\lambda_k) \left((A_k - 3\lambda_k)(A_k + D_k - 3\lambda_k) - 2B_k^2 \right) \quad (\text{C.3})$$

whose eigenvalues are:

$$\begin{aligned}
\lambda_{k,1}^{(3)} &= \frac{1}{3}(A_k - D_k), \\
\lambda_{k,2}^{(3)} &= \frac{1}{6} \left(2A_k + D_k - \sqrt{D_k^2 + 8B_k^2} \right), \\
\lambda_{k,3}^{(3)} &= \frac{1}{6} \left(2A_k + D_k + \sqrt{D_k^2 + 8B_k^2} \right), \\
\lambda_{k,j}^{(3)} &= 0, \quad j = 4, 5, 6.
\end{aligned} \tag{C.4}$$

For class 2, we have the following characteristic equation

$$\begin{aligned}
\mathcal{P}_2^{(3)}(\lambda_k) &= \frac{1}{3^3} \lambda_k^3 \left(-A_k^3 + 9A_k^2 \lambda_k + A_k (D_k^2 - 27\lambda_k^2 + B_k^2 + F_k^2) \right. \\
&\quad \left. + 27\lambda_k^3 - 3\lambda_k (D_k^2 + B_k^2 + F_k^2) - 2D_k B_k F_k \right).
\end{aligned} \tag{C.5}$$

For this equation the analytical eigenvalues are more complex so we do not report them explicitly. Finally, for class 3 we have the following characteristic equation

$$\mathcal{P}_8^{(3)}(\lambda_k) = -\frac{1}{27} \lambda_k^3 (A_k + 2D_k - 3\lambda_k)(-A_k + D_k + 3\lambda_k)^2 \tag{C.6}$$

whose eigenvalues are:

$$\begin{aligned}
\lambda_{k,1}^{(3)} &= \frac{1}{3}(A_k - D_k), \\
\lambda_{k,2}^{(3)} &= \frac{1}{3}(A_k - D_k), \\
\lambda_{k,3}^{(3)} &= \frac{1}{3}(A_k + 2D_k), \\
\lambda_{k,j}^{(3)} &= 0, \quad j = 4, 5, 6.
\end{aligned} \tag{C.7}$$

3. Causal order $m = 4$

The characteristic equation for the class 1 of quantum switch matrices with $m = 4$ causal orders is

$$\begin{aligned}
\mathcal{P}_1^{(4)}(\lambda_k) &= \frac{1}{4^4} \lambda_k^2 \left(A_k^2 + A_k(-8\lambda_k + B_k + F_k) - D_k^2 + 16\lambda_k^2 - B_k^2 - 2D_k B_k \right. \\
&\quad \left. - 4\lambda_k(B_k + F_k) + B_k F_k \right) \times \left(A_k^2 - A_k(8\lambda_k + B_k + F_k) - D_k^2 - B_k^2 \right. \\
&\quad \left. + B_k(2D_k + 4\lambda_k + F_k) + 4\lambda_k(4\lambda_k + F_k) \right)
\end{aligned} \tag{C.8}$$

whose eigenvalues are:

$$\begin{aligned}
\lambda_{k,1}^{(4)} &= \frac{1}{8} (2A_k - \gamma_k - B_k - F_k), \\
\lambda_{k,2}^{(4)} &= \frac{1}{8} (2A_k + \gamma_k - B_k - F_k), \\
\lambda_{k,3}^{(4)} &= \frac{1}{8} (2A_k - \gamma_k + B_k + F_k), \\
\lambda_{k,4}^{(4)} &= \frac{1}{8} (2A_k + \gamma_k + B_k + F_k), \\
\lambda_{k,j}^{(4)} &= 0, \quad j = 5, 6.
\end{aligned} \tag{C.9}$$

where $\gamma_k = \sqrt{4D_k^2 + 5B_k^2 - 8D_k B_k - 2B_k F_k + F_k^2}$. For the class 2 we have the following characteristic equation

$$\begin{aligned}
\mathcal{P}_3^{(4)}(\lambda_k) &= \frac{1}{4^4} \lambda_k^2 (A_k - D_k - 4\lambda_k) \left(A_k^3 + A_k^2 (D_k - 12\lambda_k) \right. \\
&\quad \left. - A_k (2D_k^2 + 8D_k \lambda_k - 48\lambda_k^2 + 2B_k^2 + F_k^2) + 16D_k \lambda_k^2 - 64\lambda_k^3 \right. \\
&\quad \left. + 4\lambda_k (2(D_k^2 + B_k^2) + F_k^2) + D_k F_k (4B_k - F_k) \right)
\end{aligned} \tag{C.10}$$

For this equation the analytical eigenvalues have complex expressions, thus we do not report them explicitly. For class 3, we have the following characteristic equation

$$\begin{aligned} \mathcal{P}_5^{(4)}(\lambda_k) = & \frac{1}{4^4} \lambda_k^2 (A_k - D_k - 4\lambda_k + B_k - F_k) \\ & \times (A_k + D_k - 4\lambda_k - B_k - F_k)(A_k - D_k - 4\lambda_k - B_k + F_k) \\ & \times (A_k + D_k - 4\lambda_k + B_k + F_k) \end{aligned} \quad (\text{C.11})$$

whose eigenvalues are:

$$\begin{aligned} \lambda_{k,1}^{(4)} &= \frac{1}{4}(A_k - D_k + B_k - F_k), \\ \lambda_{k,2}^{(4)} &= \frac{1}{4}(A_k + D_k - B_k - F_k), \\ \lambda_{k,3}^{(4)} &= \frac{1}{4}(A_k - D_k - B_k + F_k), \\ \lambda_{k,4}^{(4)} &= \frac{1}{4}(A_k + D_k + B_k + F_k), \\ \lambda_{k,j}^{(4)} &= 0, \quad j = 5, 6. \end{aligned} \quad (\text{C.12})$$

4. Causal order $m = 5$

The characteristic equation for quantum switch matrices with $m = 5$ causal orders is

$$\begin{aligned} \mathcal{P}^{(5)}(\lambda_k) = & -\frac{1}{5^5} \lambda_k (A_k - D_k - 5\lambda_k + B_k - F_k) \\ & \times (A_k - D_k - 5\lambda_k - B_k + F_k) \\ & \times (\xi_k + \lambda_k \beta_k + \lambda_k^2 (75A_k + 50D_k) - 125\lambda_k^3) \end{aligned} \quad (\text{C.13})$$

where $\xi_k = A_k^3 + 2A_k^2 D_k - A_k (D_k^2 + 3B_k^2 + 2B_k F_k + F_k^2) + 2D_k (-D_k^2 + B_k^2 + 2B_k F_k)$, and $\beta_k = -15A_k^2 - 20A_k D_k + 5(D_k^2 + 3B_k^2 + 2B_k F_k + F_k^2)$.

5. Causal order $m = 6$

The characteristic equation for quantum switch matrices with $m = 5$ causal orders is

$$\begin{aligned} \mathcal{P}^{(6)}(\lambda_k) = & \frac{1}{6^6} (A_k + 2D_k - 6\lambda_k - 2B_k - F_k) \\ & \times (A_k + 2D_k - 6\lambda_k + 2B_k + F_k)(-A_k + D_k + 6\lambda_k + B_k - F_k)^2 \\ & \times (-A_k + D_k + 6\lambda_k - B_k + F_k)^2 \end{aligned} \quad (\text{C.14})$$

and eigenvalues are

$$\begin{aligned} \lambda_{k,1}^{(6)} &= \frac{1}{6}(A_k - D_k + B_k - F_k), \\ \lambda_{k,2}^{(6)} &= \frac{1}{6}(A_k - D_k + B_k - F_k), \\ \lambda_{k,3}^{(6)} &= \frac{1}{6}(A_k + 2D_k - 2B_k - F_k), \\ \lambda_{k,4}^{(6)} &= \frac{1}{6}(A_k - D_k - B_k + F_k), \\ \lambda_{k,5}^{(6)} &= \frac{1}{6}(A_k - D_k - B_k + F_k), \\ \lambda_{k,6}^{(6)} &= \frac{1}{6}(A_k + 2D_k + 2B_k + F_k). \end{aligned} \quad (\text{C.15})$$

Appendix D: Analytical expressions for the Holevo capacity for $m=6$ causal orders

By substituting the matrix elements (3) in the eigenvalues (C 5) we found the eigenvalues $\lambda_{k,s}^{(6)}$ in terms of depolarizing parameter q

$$\begin{aligned}
\lambda_{k,1}^{(6)} &= \frac{1}{6d^2}(q-1)^2(3q+1)(d-k), \\
\lambda_{k,2}^{(6)} &= \frac{1}{6d^2}(q-1)^2(3q+1)(d-k), \\
\lambda_{k,3}^{(6)} &= \frac{1}{6d^3}(q-1)^2(d^2+dk(2-3q)+3(q-1)), \\
\lambda_{k,4}^{(6)} &= -\frac{1}{6d^2}(q-1)^3(d-k), \\
\lambda_{k,5}^{(6)} &= -\frac{1}{6d^2}(q-1)^3(d-k), \\
\lambda_{k,6}^{(6)} &= \frac{1}{6d^3}(6d^3kq^3+d^2(-10q^3+3q^2+6q+1) \\
&\quad +dk(7q+2)(q-1)^2-3(q-1)^3).
\end{aligned} \tag{D.1}$$

Substituting the above eigenvalues in equation (5), we found that the entropy H^{\min} is given by

$$\begin{aligned}
H^{\min} &= -\frac{1}{6d^3} \left[(d-1)(1-q)^2(d-3q+3) \log \left(\frac{(d-1)(1-q)^2(d-3q+3)}{6d^3} \right) \right. \\
&\quad + 2(d-1)d(1-q)^3 \log \left(\frac{(d-1)(1-q)^3}{6d^2} \right) \\
&\quad + 2(d-1)d^2(1-q)^3 \log \left(\frac{(1-q)^3}{6d} \right) \\
&\quad + 2(d-1)d(3q+1)(1-q)^2 \log \left(\frac{(d-1)(1-q)^2(3q+1)}{6d^2} \right) \\
&\quad + 2(d-1)d^2(3q+1)(1-q)^2 \log \left(\frac{(1-q)^2(3q+1)}{6d} \right) \\
&\quad + (d-1)(1-q)^2(d^2+3q-3) \log \left(\frac{(1-q)^2(d^2+3q-3)}{6d^3} \right) \\
&\quad + (d-1)(1-q)(d^2(2q+1)(5q+1)+3(1-q)^2) \\
&\quad \times \log \left(\frac{(1-q)(d^2(2q+1)(5q+1)+3(1-q)^2)}{6d^3} \right) \\
&\quad + (6d^3q^3+d^2(2q+1)(5q+1)(1-q)+d(7q+2)(1-q)^2+3(1-q)^3) \\
&\quad \times \log \left(\frac{1}{6d^3} (6d^3q^3+d^2(2q+1)(5q+1)(1-q) \right. \\
&\quad \left. \left. +d(7q+2)(1-q)^2+3(1-q)^3) \right) \right]
\end{aligned} \tag{D.2}$$

$$\tilde{\rho}_c = \begin{pmatrix} \alpha & \beta & \beta & \gamma & \gamma & \delta \\ \beta & \alpha & \gamma & \delta & \beta & \gamma \\ \beta & \gamma & \alpha & \beta & \delta & \gamma \\ \gamma & \delta & \beta & \alpha & \gamma & \beta \\ \gamma & \beta & \delta & \gamma & \alpha & \beta \\ \delta & \gamma & \gamma & \beta & \beta & \alpha \end{pmatrix}, \tag{D.3}$$

where the matrix elements are

$$\alpha = \frac{1}{6} (q^3 + 3q^2(1-q) + (1-q)^3 + 3q(1-q)^2), \tag{D.4}$$

$$\beta = \frac{1}{6d^2} (d^2q^3 + 3d^2q^2(1-q) + 2d^2q(1-q)^2 + (1-q)^3 + q(1-q)^2), \tag{D.5}$$

$$\gamma = \frac{1}{6d^2} (d^2q^3 + 3d^2q^2(1-q) + d^2q(1-q)^2 + (1-q)^3 + 2q(1-q)^2), \tag{D.6}$$

$$\delta = \frac{1}{6d^2} (d^2q^3 + 3d^2q^2(1-q) + (1-q)^3 + 3q(1-q)^2). \tag{D.7}$$

The entropy $H(\tilde{\rho}_c)$ for the output state of the control $\tilde{\rho}_c$ can be obtained from $H(\tilde{\rho}_c) = -\sum_{r=1}^6 \lambda_r^{(6)} \log(\lambda_r^{(6)})$, where $\lambda_r^{(6)}$ are the eigenvalues of matrix (D.3) (see Appendix D). Likewise in Appendix D, we give an analytical expression for $H(\tilde{\rho}_c)$, see equation (D.10).

The eigenvalues for the matrix of the output state of the control $\tilde{\rho}_c$ are

$$\begin{aligned}\lambda_1^{(6)} &= \alpha + \beta - \gamma - \delta, \\ \lambda_2^{(6)} &= \alpha + \beta - \gamma - \delta, \\ \lambda_3^{(6)} &= \alpha - 2\beta + 2\gamma - \delta, \\ \lambda_4^{(6)} &= \alpha - \beta - \gamma + \delta, \\ \lambda_5^{(6)} &= \alpha - \beta - \gamma + \delta, \\ \lambda_6^{(6)} &= \alpha + 2\beta + 2\gamma + \delta.\end{aligned}\tag{D.8}$$

By substituting the matrix elements (3) in these eigenvalues, we found them in terms of depolarizing parameter q

$$\begin{aligned}\lambda_{k,1}^{(6)} &= \frac{(d^2-1)(q-1)^2(3q+1)}{6d^2}, \\ \lambda_{k,2}^{(6)} &= \frac{(d^2-1)(q-1)^2(3q+1)}{6d^2}, \\ \lambda_{k,3}^{(6)} &= \frac{(d^2-1)(q-1)^2}{6d^2}, \\ \lambda_{k,4}^{(6)} &= -\frac{(d^2-1)(q-1)^3}{6d^2}, \\ \lambda_{k,5}^{(6)} &= -\frac{(d^2-1)(q-1)^3}{6d^2}, \\ \lambda_{k,6}^{(6)} &= \frac{1}{6} \left(\frac{(q-1)^2(4q+5)}{d^2} - 4q^3 + 3q^2 + 6q + 1 \right).\end{aligned}\tag{D.9}$$

By using these eigenvalues we found that the entropy of the output state of the control system is given by

$$\begin{aligned}H(\tilde{\rho}_c) &= -\frac{1}{6d^3} \left[(d^2-1)(q-1)^2 \log \left[\frac{(d^2-1)(q-1)^2}{6d^2} \right] \right. \\ &\quad + 2(d^2-1)(q-1)^2 \left((1-q) \log \left[-\frac{(d^2-1)(q-1)^3}{6d^2} \right] \right. \\ &\quad \left. \left. + (3q+1) \log \left[\frac{(d^2-1)(q-1)^2(3q+1)}{6d^2} \right] \right) \right. \\ &\quad \left. + (d-1)(q-1)(d^2(2q+1)(5q+1) + 3(q-1)^2) \right. \\ &\quad \left. \times \log \left[-\frac{(q-1)(d^2(2q+1)(5q+1) + 3(q-1)^2)}{6d^3} \right] \right. \\ &\quad \left. + 2(d^2(q((3-4q)q+6) + 1) + (q-1)^2(4q+5)) \right. \\ &\quad \left. \times \log \left[\frac{1}{6} \left(\frac{(4q+5)(q-1)^2}{d^2} + q((3-4q)q+6) + 1 \right) \right] \right]\end{aligned}\tag{D.10}$$